KTH Royal Institute of Technology

Modern Physics Lab Report

Atomic Nucleus

Authors:
Kevin Mead   871020-3277
Zhenping Lin 921106-T065

Lab Instructors:
Victor Mikhalev
Edvin Sidebo

May 12, 2014

Contents

1   Introduction

In this lab, we studied the radioactive materials Cesium-137 and Strontium-90. Like all radioactive materials, they have unstable nuclei and decay over time through different particle emissions. There are three main decay processes: alpha, beta, and gamma. This lab focuses on beta decay and evaluates the ability of these particles to penetrate through both aluminium and plastic.

2   Theory

In both of these radioactive isotopes, beta and gamma decay are present. The beta decay in Cesium and Strontium are both β^- decay, as opposed to β^+, and is given by

$$^A_Z P \rightarrow_{Z-1} ^A D + \beta^- + \bar{\nu}_e$$

where P and D represent the parent and daughter atoms and $\bar{\nu}_e$ is an anti-neutrino. The anti-neutrino is important because it shares the total energy with the beta particle. This leads to a continuous distribution of energies instead of discrete values, see Figure 1.

Figure 2 shows the beta decay of cesium with probabilities of each process. Each of these energies must be seen as the maximum energy a beta particle can have because it shares the total energy with an anti-neutrino. From these energies and associated probabilities, we can expect an energy distribution containing one gaussian distribution and two beta distributions with different maximum energy values. Internal conversion occurs 10% of the time at an excited state of Barium, $E = 661.7$ keV in Figure 2. The other 90% of the time, gamma rays will be emitted. Internal conversion means that an orbiting electron receives the excess energy from a transition between states in the same nucleus $E = 661.7$ keV $- E_b$, where $E_b = 37.441$ keV is the binding energy of the electron. It is emitted with an exact amount of energy every time, $E = 624.3$ keV. However, the collected data will be a normally distributed because of the errors in the measurement equipment and the different path lengths for each electron due to scattering.

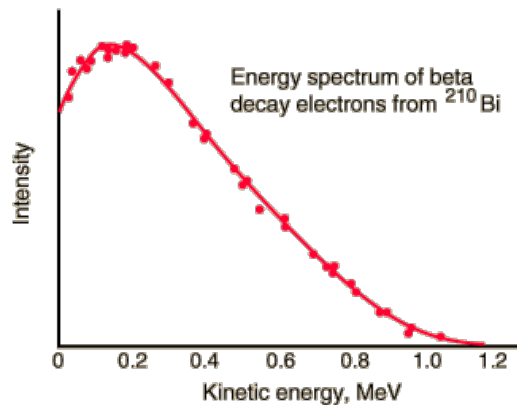In Figures 2, 3, and 4, I(%) is the radiation intensity and indicates the probability of
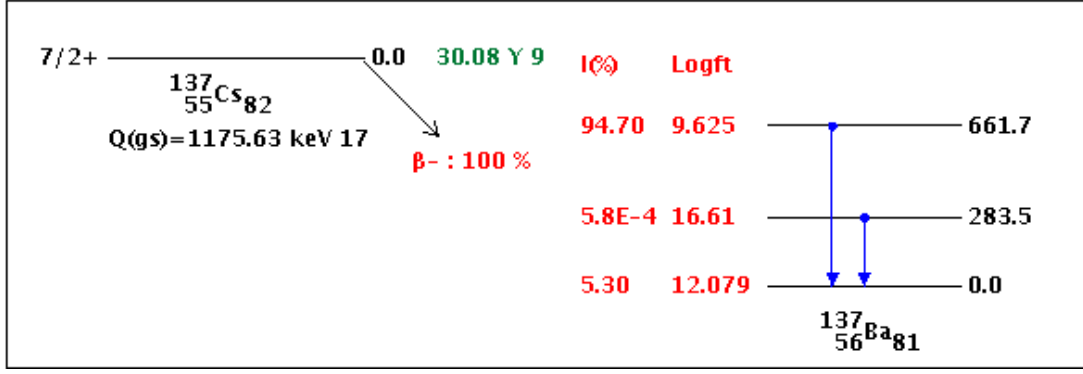

Figure 1: General beta decay energy distribution[1]
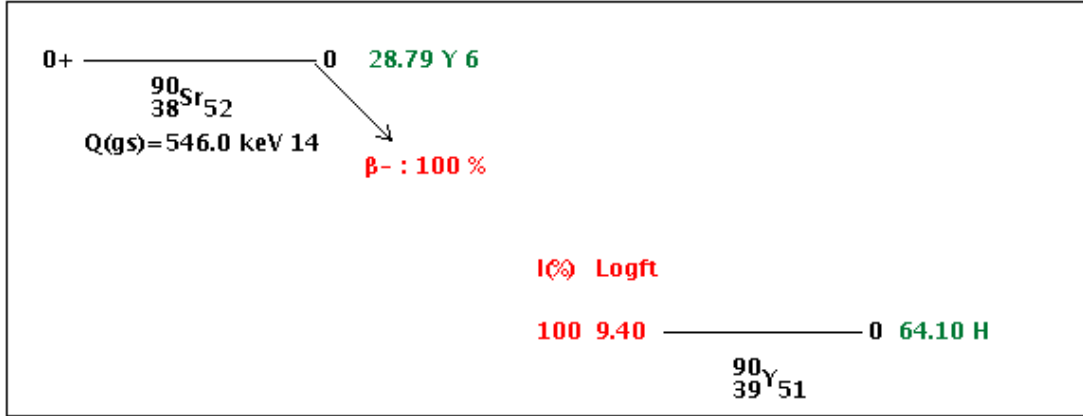
Figure 2: Decay Scheme of ^{137}Cs.[2]

Figure 3: Decay Scheme of Strontium

occurence. Logft is given by, $\log(f(Z, E_0)t_{1/2})$, where $f(Z, E_0)$ is the fermi integral, E_0 is the end point energy, and $t_{1/2}$ is the half-life. This value classifies β transitions and depends on the probability of decay, half-life, and energy.[2]

A similar beta decay process occurs for Strontium, except it decays through two elements before becoming stable. Both of these decay processes emit beta particles, but does not have internal conversion. First, Strontium decays to Yttrium, ^{90}Y, another radioactive isotope (see Figure 3). Yttrium then decays to a stable isotope of Zirconium, ^{90}Zr (see Figure 4).

From this energy distribution, we can determine the beta particles ability to penetrate materials and in this experiment we will use aluminium and plastic. We adjust the thickness of the material and the material to determine a thickness needed to stop beta particles of a certain energy. Every time we add thickness to the materials, we expect the energy distributions to shift towards lower energies. We expect a shift towards lower energies because they will lose energy due to elastic collisions and rarely will they reflect 180°. On the other hand, photons will either become absorbed, reflected, or transmitted. The energy wouldn't shift towards lower energies, but the number of counts collected would decrease with more sheets.
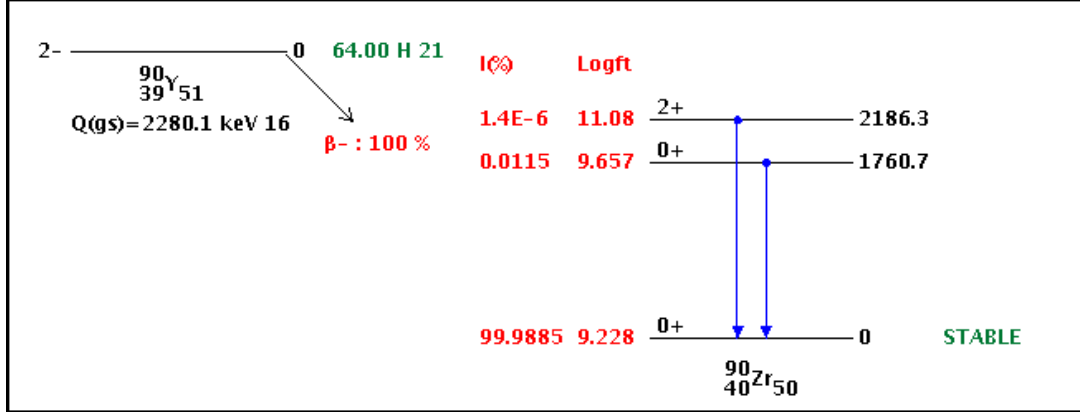
3

Figure 4: Decay Scheme of Yttrium. Two of the three decay processes shown have extremely low probabilities ($\ll 1\%$) and therefore, the only process considered has an energy, E = 2280.1 keV.

Channel Number	Corresponding Energy
0	0 eV
1838	624.3 keV

Table 1: The values we used to calibrate our system in order to relate channel numbers to energy values.

3   Experimental Setup

The two main decay processes in this experiment are gamma and beta. Since we would only like to study beta decay, we have to eliminate the detection of gamma particles. Gamma particles penetrate materials much further than beta particles. By choosing the scintillator in configuration 2, we have a smaller distance over which to absorb and detect radiation. Therefore, this scintillator will detect the beta particles and allow the majority of gamma particles to pass through undetected. It takes more material to stop gamma particles than electrons because gamma particles have a lower probability to interact with materials. This allows them to travel large distances without any interactions(or loss in energy).

To calibrate the scintillator, we used the discrete energy value given from Cesium's internal conversion, $E = 624.3$ eV. Table 1 shows the values we used to calibrate our system from channel numbers to energy values. The naive assumption was made that the zero channel corresponds to zero energy because we did not have any other known values like the discrete energy given from ^{137}Cs. This possible source of error is addressed in Section 6, Discussion/Conclusion.

4   Experimental Method

The description below describes our procedure after calibration of the equipment (n goes from $0 \to 6$ for aluminum and $0 \to 5$ and 7, for plastic). For plastic, $n = 6$ was skipped only because time was limited.

1. Place n sheets of absorbing material (aluminum or plastic) between ^{137}Cs and the detector.

2. Run PC program Multi Channel Analyser Tukan to collect a set number of counts for each measurement. The measurement with aluminum did not use this criteria, only plastic.

3. Estimate peak center and error by taking the average of the left and right peak estimations.

4. Obtain list of energies and thicknesses of absorbing material.

5. Estimate the thickness needed to stop beta particles ($E \approx 0$) using a linear approximation.

6. Estimate and plot $R(E) = \mathrm{k}E^{\mathrm{B}}$, where k and B are constants and $R(E)$ is the length of material needed to stop an electron of energy E. Estimation of the stopping distance is done by assuming a linear relationship between number of sheets and electron energy. As more sheets are added, the energies of the collected electrons become smaller and less frequent as they are being scattered from collisions with the absorbing material.

7. Compare results with similar experiments.[3,4]

5   Results

The peaks of each measurement was recorded in Table 2 and Figure 5 and 6 show the energy distributions from both absorbers while collecting data from ^{137}Cs. The electron range, $R(E)$, is interpolated using a linear fit of thickness as a function of energy with the weights $1/\sigma^2$ from Table 2. We fit the function to the equation $R(E) = kE^B$, using a least squares fit. We used a change of variables to transform our equation into a linear problem,

$$
\begin{aligned}
y &= mx + c \\
\ln(R(E)) &= y \quad \mathrm{d}y = \mathrm{d}R/R \\
\ln(E) &= x \quad \mathrm{d}x = \mathrm{d}E/E \\
\ln(k) &= c \quad \mathrm{d}c = \mathrm{d}k/k \\
B &= m \quad \mathrm{d}m = \mathrm{d}B
\end{aligned}
$$

Our chi-squared value for aluminum and plastic are 398 and 33.4 where $N - 2 = 5$. For a good fit, we want $\chi^2 \approx N - 2$. If $\chi^2 \gg N - 2$, it suggests that we are either using the wrong function or our error bars are too small. If $\chi^2 \ll N - 2$, it suggests that the data fits so well that maybe our error bars are too large.[5] We believe the function fit to
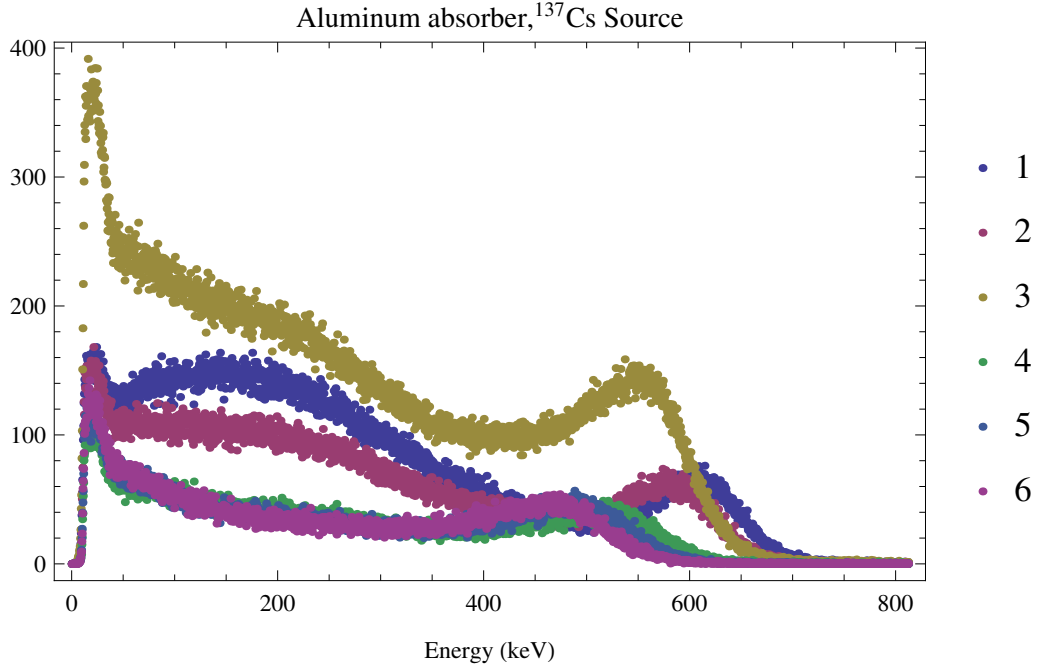
Figure 5: The peaks also shift towards lower energies for aluminum. In order to normalize their intensities, the data for sheets 4,5, and 6 have a constraint on the maximum number of counts collected. The numbers 1-6 in the plot above and 1-5,7 in Figure 6 represent the number of sheets between the radioactive isotope and the scintillator.

n	Aluminum (peak $\pm \sigma$) [keV]	Thickness (cm)	Plastic (peak $\pm \sigma$) [keV]	Thickness (cm)
0	624.259 ± 3	0	624.259 ± 3	0
1	601 ± 4	0.0054	591.5 ± 6.5	0.01
2	577.5 ± 1.5	0.0108	567.5 ± 5.5	0.02
3	550.5 ± 7.5	0.0162	537.5 ± 6.5	0.03
4	505.5 ± 1.5	0.0216	501 ± 9	0.04
5	470.5 ± 8.5	0.027	470.5 ± 4.5	0.05
6	450.5 ± 10.5	0.0324	*N/A*	*N/A*
7	*N/A*	*N/A*	413 ± 13	0.07

Table 2: Data collected shows our estimated peaks with standard deviations from taking the average of two possible peaks, one low energy and one high energy.
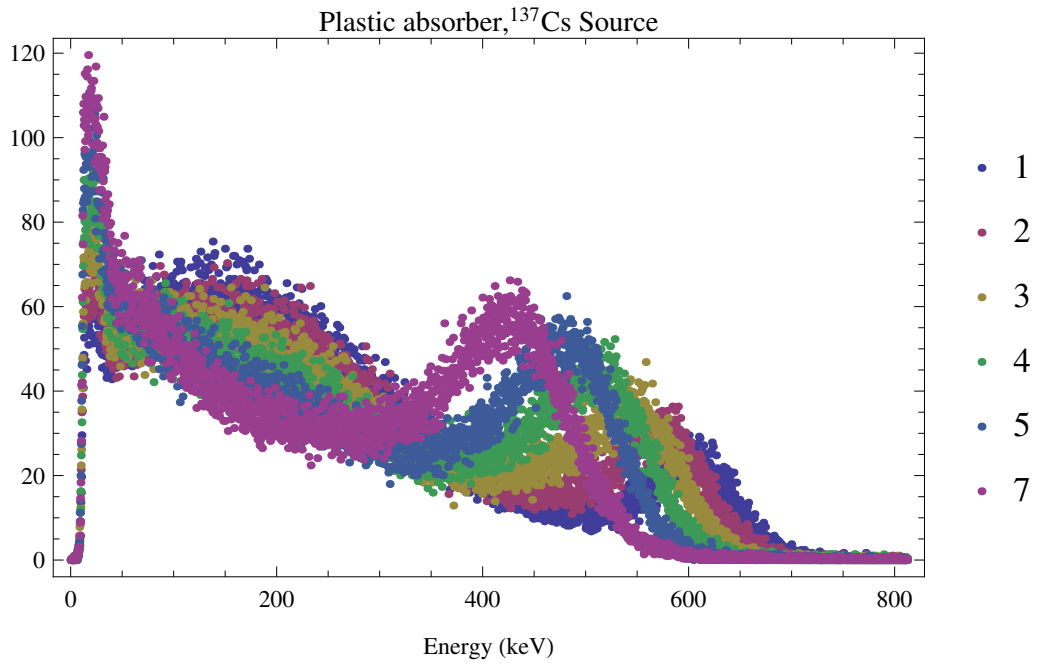
Figure 6: The peak of ^{137}Cs shifts towards lower energies as more absorbers are added. The system was programmed to run until a set number of counts were collected. The sum of three spectrums shown above contain: the beta spectrum of max energy 1175.63 keV (5%), the beta spectrum of max energy 513.93 keV (95%), and the gaussian distribution with a center at 624.3 keV (10%).

our data sufficiently describes the range in this domain, but not outside of it. The values for k and B of aluminium are obtained are: $k = 0.443 \pm 0.001$ and $B = 0.978 \pm 0.006$. The values for k and B of plastic are: $k = 0.369 \pm 0.002$ and $B = 0.996 \pm 0.007$. These error bars for aluminum and plastic are significantly too small, which also agrees with analysis of the chi-squared value.

$R(E)$ has units of g/cm^2, making the values independent of the absorbing material. Figure 7 shows our results compared to two other credible sources[3,4], each with uncertainties around 5%.
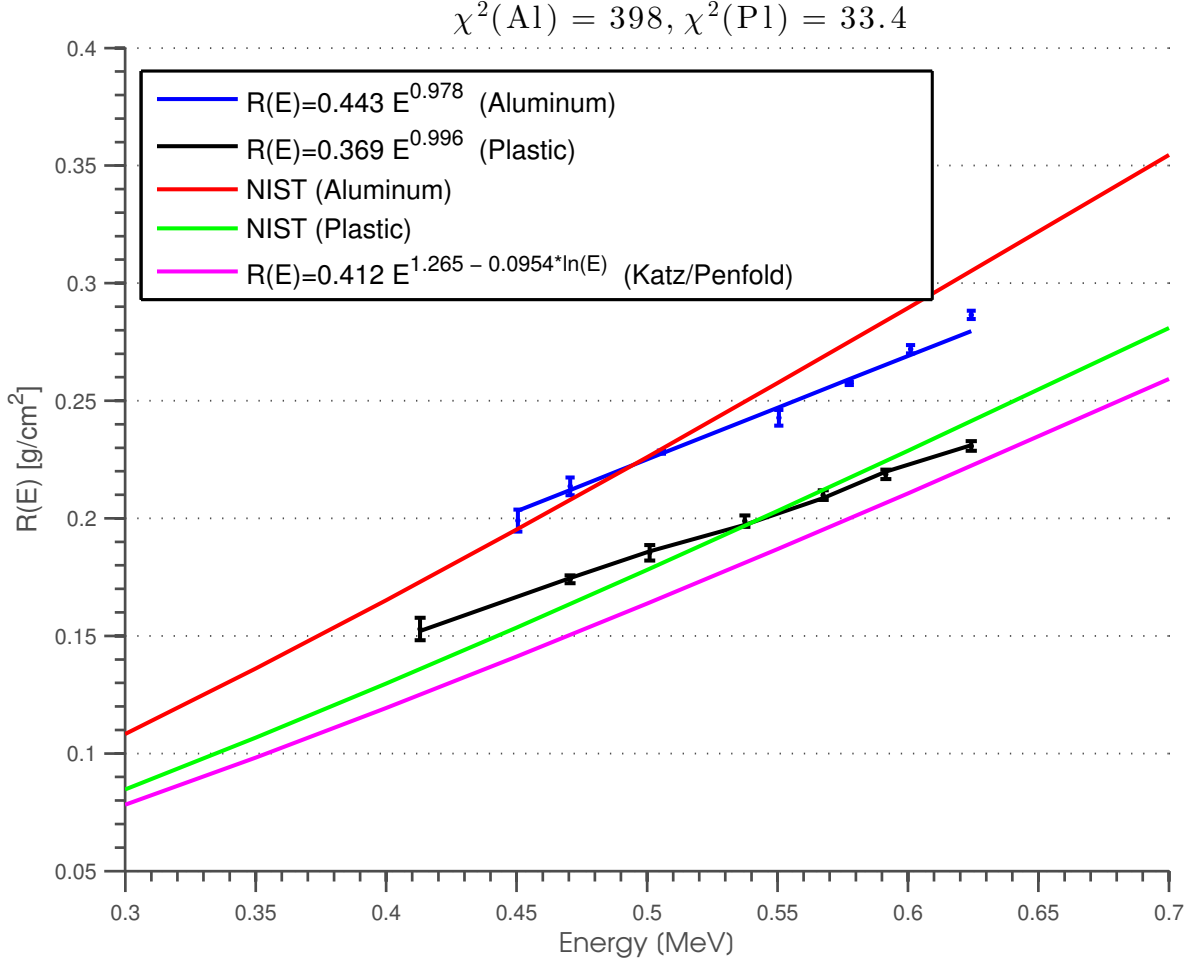

Figure 7: Comparison of data from aluminum and plastic with accepted values.

6 Discussion/Conclusion

The relative intensities between each plot of Figure 5 do not give as much insight as those in Figure 6 because the counts collected were not declared beforehand. We realised the necessity of this criteria and set it for all the collected data with plastic. The data we collected agrees within our calculated error of uncertainty for higher energies, but for lower energies, our model gets progressively worse.

Aluminum		Plastic	
$\delta R(E)$ $[\frac{\text{mg}}{\text{cm}^2}]$	δE [keV]	$\delta R(E)$ $[\frac{\text{mg}}{\text{cm}^2}]$	δE [keV]
1.77	4.0	2.03	5.5
1.77	4.0	2.03	5.5
0.66	1.5	2.03	5.5
3.32	7.5	2.40	6.5
0.66	1.5	3.32	9.0
3.77	8.5	1.66	4.5
4.65	10.5	4.80	13.0

Table 3: The uncertainties in the range is calculated from our uncertainties in energy peaks using equation,[6] $\delta R(E) = |k|\delta E$. This equates to about 1% uncertainty.

We do expect to have a larger deviation at lower energies because we assumed a linear model to simplify calculations. It is also evident from both sources that the relationship isn't exactly linear, but roughly follows this semi-empirical equation from Katz and Penfold,[3]

$$R(E) = 0.412E^{1.265-0.0954\ln(E)} \tag{1}$$

Comparing this to our approximation, $R(E) = 0.443E^{0.978}$ for aluminium and $0.369E^{0.996}$ for plastic, we are satisfied with the results as they are good approximations. It is good that the aluminum and plastic fitted equations agree with their NIST counterparts, even though the units for $R(E)$ is supposed to make it independent of the absorbing material. To calculate the errors, we used the equation,[6] $\delta R(E) = |k|\delta E$ and we know δE from Table 2. Note that in this experiment, we assume that the uncertainty in the thickness of aluminium and plastic is negligible.

In both Equation (1) and our approximation, $R(E)$ is in units of $[\frac{\text{g}}{\text{cm}^2}]$ and E is in [MeV]. The uncertainty of our data is shown in Table 3. Berger states the uncertainty in measurements increases for lower energies,

$$\frac{\delta R(E)}{R(E)} = \begin{cases} 5 \text{ to } 10 \ \% \text{ if } 10 \text{ keV} < E < 100 \text{ keV} \\ 1 \text{ to } 2 \ \% \text{ if } E > 100 \text{ keV} \end{cases} \tag{2}$$

for the reason that at lower energies the electron energy is not large compared to the atomic electrons and therefore, the model, lacking any electron shell corrections, becomes less accurate. Berger also states that materials of low atomic number like air or plastic, will have a higher uncertainty $\sim 10\%$. In both of our models, we estimated about 1% uncertainty, which likely means that we did not estimate our errors properly.

If we assume that our uncertainty in both E and R(E) also increase for lower energies, then our results almost agree within margins of error with the accepted model for all values of R(E) and E. We believe that the fact that the equation for R(E) is independent of material shows us that our measurements for both materials were consistent with each other because they are within our estimated margins of error. This lead us to believe that we would need a better approximation if we would want to improve our model to

T (°C)	T (K)	T (°F)	T (°R)
2.32	5.50	2.04	4.00
2.23	5.50	1.94	4.00
2.13	5.50	0.76	1.50
2.40	6.50	3.26	7.50
3.25	9.00	0.59	1.50
1.52	4.50	3.60	8.50
4.48	13.00	4.32	10.50

compare with other standards. We also believe that our uncertainty was too low and it should on the same scale as other sources, 5% to 10%.

References

[1] G. J. Neary, "The β-ray spectrum of radium e," *Proceedings of the Royal Society of London. Series A. Mathematical and Physical Sciences*, vol. 175, no. 960, pp. 71–87, 1940. [Online]. Available: http://rspa.royalsocietypublishing.org/content/175/960/71.short

[2] (2014, March). [Online]. Available: http://www.nndc.bnl.gov

[3] L. Katz and A. S. Penfold, "Range-energy relations for electrons and the determination of beta-ray end-point energies by absorption," *Rev. Mod. Phys.*, vol. 24, pp. 28–44, Jan 1952. [Online]. Available: http://link.aps.org/doi/10.1103/RevModPhys.24.28

[4] M. Berger. (2014, March) Estar, pstar, and astar: Computer programs for calculating stopping-power and range tables for electrons, protons, and helium ions (version 1.2.3). [Online]. Available: http://physics.nist.gov/Star

[5] A. Garcia, *Numerical methods for physics.* Prentice Hall, 2000.

[6] J. R. Taylor, *An Introduction to Error Analysis: The Study of Uncertainties in Physical Measurements*, 2nd ed. University Science Books, 1996.